Applied Catalysis, 42 (1988) 15–27
Elsevier Science Publishers B.V., Amsterdam — Printed in The Netherlands

Diffusion, Cracking and Coking on HZSM-5 of Various Morphologies

JOACHIM VÖLTER*, JÜRGEN CARO and MARTIN BÜLOW

Zentralinstitut für physikalische Chemie der Akademie der Wissenschaften der D.D.R., Rudower Chaussee 5, 1199 Berlin (G.D.R.)

BARBARA FAHLKE

Zentralinstitut für anorganische Chemie der Akademie der Wissenschaften der D.D.R., Rudower Chaussee 5, 1199 Berlin (G.D.R.)

and

JÖRG KÄRGER and MICHAEL HUNGER

Sektion Physik der Karl-Marx-Universität Leipzig, Linnestr. 5, 7010 Leipzig (G.D.R.)

(Received 10 April 1987, accepted 10 March 1988)

ABSTRACT

Coked HZSM-5 samples of polycrystalline spherical and polyhedral morphology were studied using an NMR self-diffusion technique and n-hexane cracking. It was concluded that, in addition to the first order pores of the regular zeolite channel network, the polycrystalline grain contained second order pores. Second order pores exhibited two remarkable properties: self-diffusion was enhanced, and coke was deposited preferentially within them. The presence of empty second order pores allowed coking to occur without significant poisoning. The cracking rate decreased with increasing particle size.

INTRODUCTION

Elucidation of the mechanism of coke formation on pentasil type zeolites represents a challenging task to both basic and industrial research workers. Recently, selected problems of coke deposition on HZSM-5 have been resolved, e.g. the interdependence of coking and deactivation rates [1–3], the role of zeolite pore structure in determining the chemical composition of the coke [1–3] and the poisoning of acid sites by coke [4]. Still contradictory, however, are the results from experiments examining the influence of crystal size and morphology [5] on the coking behaviour of HZSM-5 and those from experiments where the problem of where the coke is deposited are dealt with. Whereas in some previous papers HZSM-5 was assumed to produce coke preferentially on the external surface of the crystals [6, 7] recent studies give clear evidence of

0166-9834/88/$03.50 © 1988 Elsevier Science Publishers B.V.

the existence of coke inside the crystals. Such intracrystalline coke deposits in the channel network have been detected by different techniques, e.g. by a dissolution technique of the coked zeolites in hydrofluoric acid [1, 2], by changes in the ^{29}Si and ^{27}Al MAS NMR spectra of the zeolite during the generation of coke [8], by a decrease of acidity due to acid site blockage by coke [4], by a loss of sorption capacity for guest molecules on coked samples [9] and by the changes of the X-ray diffraction patterns of HZSM-5 containing coke deposits [9].

Recently we presented a new NMR method for the determination of coke positions in HZSM-5 type zeolites [10]. By measuring the influence of coke deposits on molecular self-diffusion, it is possible to distinguish between intracrystalline and surface coke. Combining this with the measurements of the chemisorption of pyridine on coked samples, via the loss of acidity, it was possible to demonstrate that coking of HZSM-5 caused a combination of pore blocking and acid site poisoning. We have continued these investigations and now present information on the influence of crystal size and morphology on the coking of HZSM-5, with special reference to the selectivity of coke formation, and coke distribution over the crystal. n-Hexane cracking at 500°C was used as the reaction for coke production. In recent literature [11–14], the cracking activity of HZSM-5 was found in general to be proportional to the concentration of lattice aluminium and hence to the Brønsted acid site density. Therefore, in our experiments we used four HZSM-5 samples of different crystal size and morphology but of comparable acidity.

Zeolite preparation

The four specimens of ZSM-5 type zeolites were prepared in the presence of TPA according to established procedures [15]. After calcination in air (550°C, 24 h), the zeolites were converted into the H-form via repeated NH_4-ion exchange (at 90°C) followed by further calcination (550°C, 2 h).

^{1}H-MAS NMR measurements

The zeolites were heated in vacuo at a heating rate of 10°C/h up to 400°C. After keeping them at the final temperature for two hours, the samples were evacuated to a pressure below 0.05 Pa. ^{1}H-MAS NMR spectra were taken at room temperature at a resonance frequency of 300 MHz using a BRUKER MSL 300. The sealed sample ampoules were spun at a rotation frequency of about 2 kHz. The total concentration of protons was determined by measuring the free induction decay after a $\pi/2$-pulse without sample spinning and by comparing its initial value with that of a standard.

Cracking and coking

Coke was deposited by n-hexane cracking at 500 °C in a fixed bed-type glass reactor at atmospheric pressure with a continuous stream of hydrogen (2 l/ $h \cdot g_{catalyst}$) saturated at 16 °C with n-hexane. The HZSM-5 zeolite (0.5 g) was supported on a glass frit. The amount of n-hexane converted into coke and volatile cracking products was determined by gas chromatography. The coke content of the zeolites was measured by combustion of the coke and micro-analysis of the products.

^{1}H-NMR diffusion measurements

The coked zeolites were heated in vacuo up to a temperature of 350 °C. Methane and propane, respectively, were admitted into the tubes, which were then sealed. The sorbed amounts of hydrocarbons were determined both volumetrically and gravimetrically. For the determination of the intracrystalline self-diffusion coefficients D_i, the r.m.s. molecular displacements $\langle \vec{r}^2(\Delta) \rangle^{1/2}$ of the sorbed molecules during an observation time Δ were measured by means of the NMR pulsed field gradient technique [16]: $D_i = \langle \vec{r}^2(\Delta) \rangle / 6 \cdot \Delta$.

Whereas diffusion obstacles such as coke deposited on the external surface of the zeolite crystal do not influence D_i, transport resistances, such as carbonaceous residues within the intracrystalline channel network, cause a severe reduction of the intracrystalline self-diffusivity D_i of sorbed guest molecules. On the other hand, NMR tracer desorption experiments give information on the fraction γ of those molecules which leave the crystals during the observation time Δ. By fitting the corresponding solution of Fick's law for diffusion-limited desorption to the tracer desorption curves, an effective diffusion coefficient D_d was determined [16, 17]. D_d is influenced by coke deposits on the external surface as well as inside the crystals. It is, however, a useful parameter for describing a desorption rate retardation due to surface barriers [18].

RESULTS AND DISCUSSION

Characterization of crystal morphology and structure

As Table 1 shows, the samples under study differed remarkably in crystal size and morphology. Sample 1, synthesized from a stirred batch, consisted of polycrystalline spherical particles with the habit of "intergrown discs" [19]. Fig. 2 gives an impression of the polycrystalline substructure of Sample 1. In contrast, Samples 2–4, obtained from an unstirred batch, were twinned polyhedral crystals of different sizes with an elongated hexagonal form [19].

The newly developed ^{1}H-MAS NMR technique allowed protons of different acidity to be distinguished [20]. By applying this method, the concentrations

TABLE 1

Characterization of the HZSM-5 type zeolites under study

	Sample No.			
	1	2	3	4
Mean crystal size/μm	6.5* 0.5**	8.5	14	28
Crystal shape	Polycrystalline spherical grains	Polyhedral crystals, twinned	Polyhedral crystals, twinned	Polyhedral crystals, twinned
Silicon:aluminium ratio of the starting batch in zeolite synthesis	35	35	30	35
Silicon:aluminium ratio of the zeolite lattice as determined from ^{1}H-MAS NMR	31	31	29	33
Concentration of Brønsted acid hydroxyl groups as measured by ^{1}H-MAS NMR/10^{19} g^{-1}	30	30	32	28
Concentration of non-acidic internal silanol groups as lattice defects/ 10^{19} g^{-1}	38	47	41	38

*Spheres.
**Thickness of a disc.

of Brønsted acid protons formed by bridging hydroxyl groups and catalytically non-active silanol groups were determined. Due to the identical silicon-to-aluminium ratio in the starting batch, the resulting HZSM-5 samples were of comparable silicon:aluminium ratio. Sample 4 was no exception in spite of the less alkaline synthesis conditions [21]. Furthermore, the samples also contained remarkable concentrations of non-acidic silanol groups. Due to non-intact Si–O–Si bonds, up to 5% of the lattice silicon was found to be present as Si–OH groups. This result was in accordance with our previous finding [22] that HZSM-5 type zeolites prepared using TPA as a template had high concentrations of defect centres within the structure. Due to the consistent synthesis procedure employed, all the samples investigated in our work possessed similar concentrations of internal silanol groups.

Diffusion in coked HZSM-5 of different morphology

Firstly, the self-diffusion of methane and propane in the polycrystalline grains (Sample 1) and in the polyhedral crystals (Samples 2–4) were compared in the uncoked state. The corresponding data are given in Table 2. It follows from inspection of these data that the intracrystalline self-diffusion coefficient in the polycrystalline grain was, by a factor of 2 to 3, higher than in the polyhedral crystals. In a previous paper [19] this experimental finding was explained by a promotion of molecular transport due to additional fast diffusion paths originating from the polycrystalline structure of the grain. Hence, the increase in diffusivity can simply be considered as a higher molecular mobility in the voids between the intergrown discs forming the substructure of the grain. Obviously, the interfacial voids between adjacent discs had the nature of transport pores. It was concluded therefore, that the polycrystalline grains contained second order pores in addition to the first order pores of the channel network of the zeolite. From this diffusion model for polycrystalline grains, an enhancement of molecular mobility with increasing observation time is to be expected. Results of corresponding experiments are displayed in Fig. 1, which revealed the self-diffusion coefficient of propane in Sample 1. For the uncoked sample, an increase of D_i was indeed observed with increasing observation time. This finding can be understood by the following mechanism. During short observation

TABLE 2

Intracrystalline self-diffusion coefficients D_i of methane and propane in HZSM-5 of different morphology (loading 2.3–2.5 molecules per 1/4 u.c., 23 °C)

Morphology	D_i (CH_4)/$m^2\,s^{-1}$	D_i (C_3H_8)/$m^2\,s^{-1}$
Polyhedral crystals	$0.8 \cdot 10^{-8}$	$1.5 \cdot 10^{-10}$
(Samples 2–4)	$2.3 \cdot 10^{-8}$	$3 \cdot 10^{-10}$

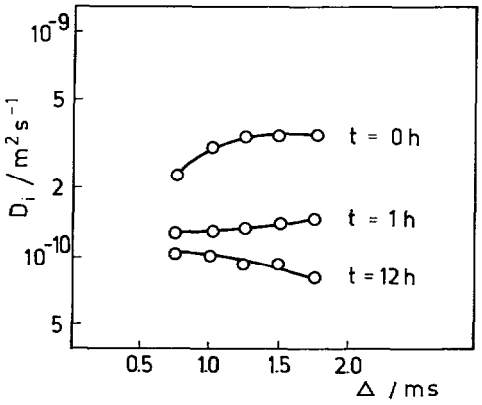


Fig. 1. Self-diffusivity D_i of propane (loading approximately 2.5 molecules per 1/4 u.c., 23°C) as a function of observation time Δ of self-diffusion for polycrystalline grains after different coking times.

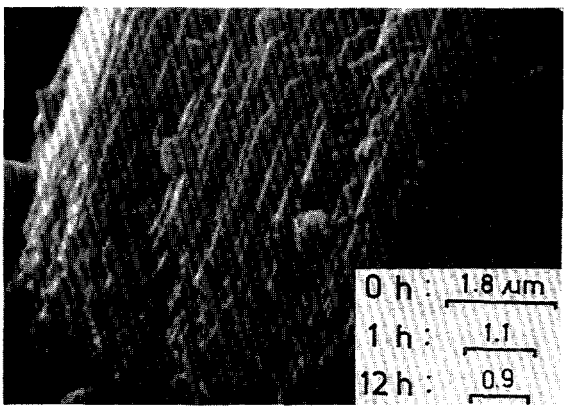


Fig. 2. SEM of Sample 1. For comparison, the reduction of the mean diffusion paths of propane sorbed after different time on stream (t) is indicated. Constant observation time $\Delta = 1.5$ ms.

times, the propane molecules move preferentially within the substructure of the polycrystalline grain. With increasing time intervals allowed for diffusion, an increasing number of molecules will enter the interspace between the discs, a region of transport enhancement, and will travel over longer distances there.

Consideration of the self-diffusivity of propane in coked Sample 1, afforded details of the peculiarities of coke formation on polycrystalline particles. Fig. 1 shows that after a coking time of 1 h only a slight increase of D_i with the observation time occurred. However, after 12 h a slight decrease was observed. This behaviour can easily be explained if one assumes that coke is preferrentially incorporated in the second order pores. This means that the interspaces between the discs progressively lose their transport promoting character. Fi-

nally, the second order pores, when filled up with coke, become a transport hindrance.

Fig. 2 shows an SEM of the external surface of Sample 1 in comparison with the mean diffusion path of sorbed propane in dependence on the coking time. It can be seen that the substructure of the grain and the mean diffusion path were indeed of the same order of magnitude.

Determination of the positions of the coke deposits by self-diffusion and desorption experiments

The reduction of molecular diffusion due to coking can be used to determine the position of the coke deposits within the intracrystalline channel network or near the external surface of the zeolite crystals. If molecular exchange between the crystals, as detected by the NMR tracer desorption technique, is limited by intracrystalline self-diffusion, the value of the thus determined tracer desorption diffusivity D_d must be equal to that of the directly measured NMR intracrystalline self-diffusion coefficient D_i. If the value of D_d is low compared with that of D_i this indicates the presence of mass transport barriers due to coke deposits near the external surface of the crystals.

As an example, Fig. 3 shows the decrease of D_i and D_d for Sample 2 as a function of time-on-stream. Despite continuous coke formation (cf. Table 2), after approximately 2 h time-on-stream, the intracrystalline mobility of the guest molecule methane remained practically constant. In contrast, the desorption rate continued to slow down, indicating an increasing transport resis-

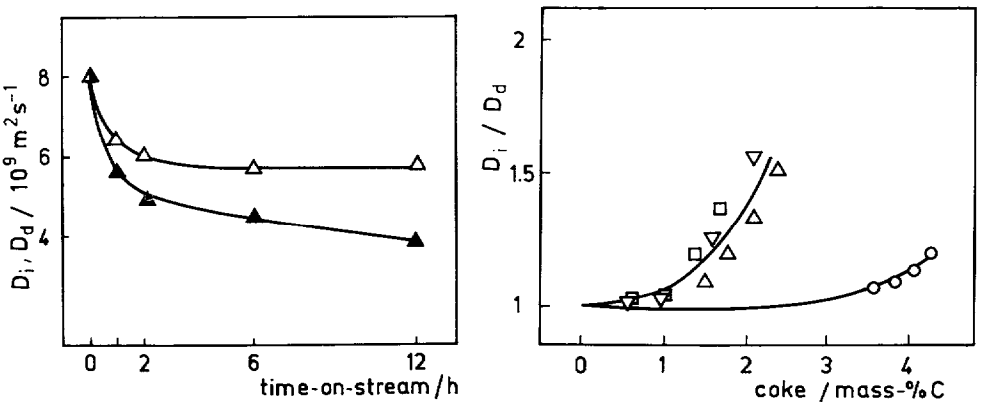


Fig. 3. NMR intracrystalline self-diffusion coefficient D_i (△) and NMR tracer desorption diffusivity D_d (▲) of methane sorbed on Sample 2 (loading approximately 2.3 molecules per 1/4 u.c., 23 °C) with increasing coking time.

Fig. 4. The dependence of the ratio of D_i/D_d on the amount of coke deposited: (○) Sample 1, (△) Sample 2, (▽) Sample 3 and (□) Sample 4.

tance near or on the external surface. Obviously, with increasing blockage of the intracrystalline channel system by coke, further coke was preferentially deposited in the outer regions of the zeolite crystals, blocking the mouths of pores.

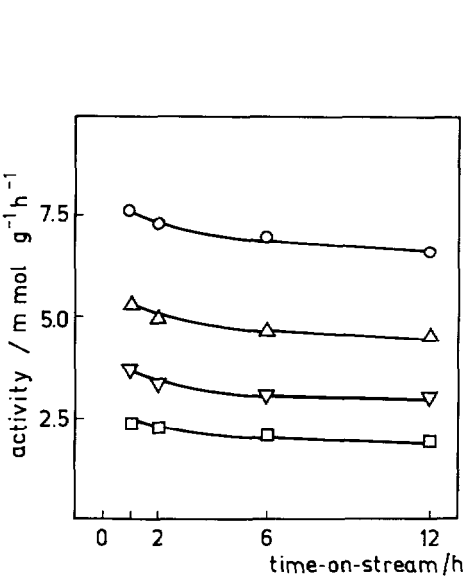
Fig 4 shows the ratio D_i:D_d for the four zeolite samples under study as a function of coke deposited. In accordance with our previous finding [10], two periods of coke formation could be distinguished. In the first period, the ratio D_i:D_d remained approximately equal to unity, thus indicating a homogeneous coke distribution over the whole crystal. In the second period, D_i:D_d increased indicating an enrichment of coke in the surface region. Surprisingly, the beginning of the second period was virtually the same for all three polyhedral crystals (Samples 2–4). However, a distinct delay of this onset was observed with the polycrystalline grain (Sample 1). Also from this experimental finding, we were led to the conclusion that there was an additional pore system inside the grain which could be filled up by coke. This additional amount of coke deposited in the second order pores caused a delay to the onset of the second period of coke formation.

Cracking on coked HZSM-5

The catalytic activity of the four samples was studied using the cracking of n-hexane as a test reaction. It is well known that this process is accompanied by severe coking of the catalysts. The cracking activity and the amount of coke deposited were determined after 1, 2, 6 and 12 h time-on-stream. New material was used each time. The activity is defined as the consumption of n-hexane. The products formed were C_1–C_4 hydrocarbons only and coke.

The cracking activities as a function of time-on-stream are shown in Fig. 5. Compared with the polycrystalline grain (Sample 1), the polyhedral crystals (Samples 2–4) were less active in the given sequence. Different activities of acid catalyzed reactions can be caused by different acid site densities provided by Brønsted acid hydroxyl groups. However, the observed sequence of activity could not be explained by the concentration of acid sites in the four samples as listed in Table 1.

The influence of reactant diffusion in the pore system could be another reason for the differences in the observed activities. Fig. 5 shows that the different cracking activities can obviously be correlated with differences between the sizes of the crystals used. This situation can be described by the Thiele modulus concept [23–25] for the reaction rate retardation due to mass transport effects. Following this concept, the activity will decrease with increasing crystal size if the Thiele modulus exceeds a limiting value. As shown by Haag et al. [24] the activity for n-hexane cracking was not affected by a change, by a factor of 50, in the ZSM-5 crystal size when the Thiele modulus $\phi = R(k/D)^{1/2} \ll 1$. Only if $\phi \gg 1$, did the reaction rate depend on the crystal radius



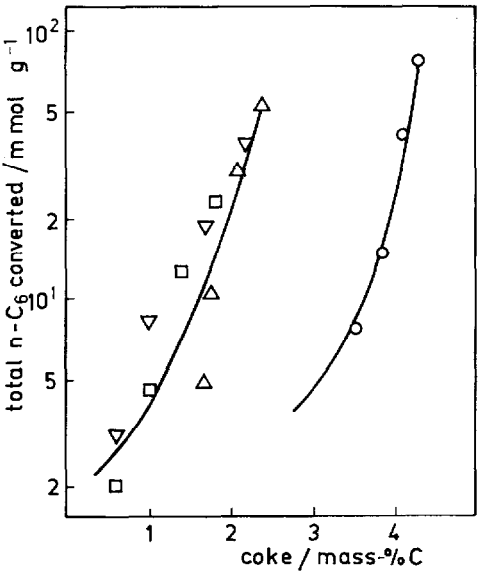


Fig. 5. Activities for n-hexane cracking at 500 °C as a function of time-on-stream (symbols as in Fig. 4).

Fig. 6. Total amount of n-hexane converted as a function of the amount of coke deposited (symbols as in Fig. 4).

TABLE 3

Amounts of coke deposited during n-hexane cracking on HZSM-5 at 500 °C

Time-on-stream (h)	Coke content (mass-% C)			
Sample No.	1	2	3	4
1	3.6	1.5	0.6	0.65
2	3.8	1.8	1.0	1.0
6	4.1	2.1	1.7	1.4
12	4.3	2.4	2.2	1.8

R, what seemed to be the case here where we used much larger crystals than those used in ref. 24. This theoretical prediction was in complete agreement with our experimental finding. The large particle size of the zeolites (cf. Table 1) caused the differences in the cracking activity due to diffusion inhibition. The very high activity of Sample 1 did not originate from the small particle size alone. As shown above, the polycrystalline grain contained second order

pores with transport promoting properties. Consequently, they diminished the limitations of mass transport imposed by the zeolite channel network.

In a simultaneous study, Herrmann et al. [26] also found a decrease of the n-hexane cracking activity as the crystal size of HZSM-5 increased. The particle size effect, however, could be overcompensated by structural irregularities. Thus, Hölderich and Riekert [27] reported lower activity for very small particles of ZSM-5 than for large crystals of ZSM-5. They assumed that the small particles contained structural imperfections or even amorphous material.

The conversion of n-hexane was accompanied by severe coking causing deactivation during time-on-stream, as seen in Fig. 5. The values for the amounts of coke deposited are listed in Table 3. It follows from inspection of this data that the initial rate of coke formation, as well as the final amount of coke deposited, was especially high on Sample 1, which was the most active one. This finding indicates a direct relation between high cracking activity and high coke production.

The relationship between the total amount of n-hexane converted and the amount of coke deposited is shown in Fig. 6. The final points of the curves represent the corresponding values of the four samples after 12 h on-stream. The shapes of the curves are remarkable. Initially a small increase in n-hexane cracking was accompanied by a large increase in coke production. Finally a large increase in cracking products was accompanied by only a small increase in coke deposition. The predominating coke production characterized the beginning of the reaction. This tendency is also seen in the data in Table 3.

Once again, the curves for Samples 2–4 were very similar. Only the curve for Sample 1 was exceptional. For this sample, the period of enhanced coking was prolonged. This exceptional behaviour corresponded very well with the diffusion peculiarities of this sample (cf. Fig. 1). Hence, the reasons for these features should be the same.

In contrast to the polyhedral crystals (Samples 2–4), the polycrystalline grain (Sample 1) could accomodate more coke, until the cracking and diffusion properties were dramatically changed. Obviously, the location of this coke was on "neutral" spots outside the channel network, i.e. in the second order pore system as detected in this sample. This conclusion agrees with the experimental finding of ref. 9. They found out that the initial rate of coke formation was higher with spherical polycrystalline particles than with polyhedral crystals.

The influence of coke deposition on the selectivity of coking is shown in Fig. 7. The selectivity was calculated as the mole ratio of n-hexane transformed into coke, divided by the amount of n-hexane converted. The selectivity curves for all four samples investigated distinctly decreased with increasing coke content. This proved that there was self-poisoning of the coking in the course of the reaction. Hence, two effects of the deposited coke were observed: the total conversion was inhibited (cf. Fig. 5) and, in addition, the selectivity of coking was inhibited. Selective blocking of the coking route could be a transport phe-

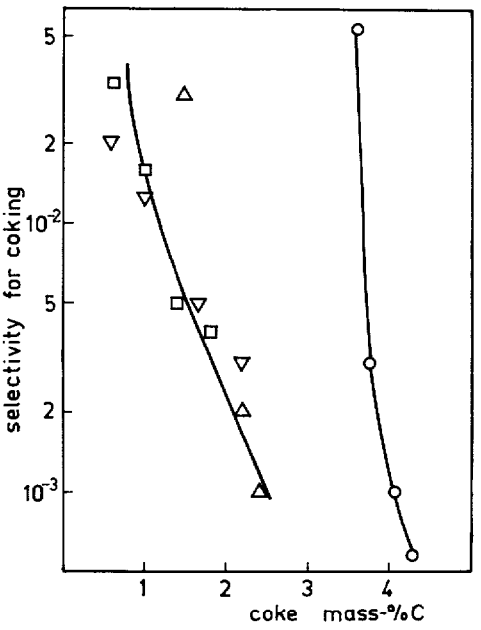


Fig. 7. The dependence of the selectivity of coke formation during n-hexane cracking at 50 °C on the amount of coke deposited (symbols as in Fig. 4).

nomenon. Coke precursors are formed inside the channel network on catalytically active sites. They move to regions where they form fixed coke deposits. This movement could increasingly be hindered as increasing amounts of coke are deposited.

The selectivity curves in Fig. 7 are very similar for Samples 2–4, but again Sample 1 behaves exceptionally. The amount of coke necessary for the same poisoning effect, i.e. for the same selectivity level, was much higher for Sample 1 than for the other samples. This was a further demonstration that the polycrystalline grains could accomodate coke on "neutral" spots in the second order pore system inside the grain.

CONCLUSIONS

(i) Polycrystalline grains of HZSM-5 exhibited enhanced diffusivity in comparison to samples of polyhedral morphology. We concluded that the grains contain second order pores, in addition to the zeolite channels which represent first order pores.

(ii) Coke is preferentially deposited in the second order pores as demonstrated by the diffusion and cracking experiments. Due to the coke deposition outside the channel network, the initial coking rate on the polycrystalline grains is higher than on the polyhedral crystals.

(iii) Diffusion and cracking experiments revealed two periods of coking. In the first period, coke was distributed homogeneously throughout the crystal. In the final period, an enrichment of the coke near the surface took place. Polycrystalline grains exhibited a prolonged first period, due to the second order pores.

(iv) The selectivity of coking in n-hexane cracking decreases with increasing coke deposition. Larger amounts of coke are necessary for poisoning of polycrystalline than for polyhedral samples. This is explained as being the result of deposition in neutral positions in second order pores.

(v) Cracking activity decreases with increasing particle size, a finding we explained as a consequence of mass transport effects.

(vi) NMR self-diffusion experiments offer a new method for detecting second order pores in polycrystalline adsorbents and catalysts.

ACKNOWLEDGEMENT

The authors wish to thank Profs. H. Pfeifer (Leipzig), G. Öhlmann (Berlin), W. Schirmer (Berlin), L.V.C. Rees (London) and Dr. K. Becker (Leuna) for stimulating discussions. Mrs. W. Ziesche (Berlin) is thanked for experimental assistance, Dr. J. Richter-Mendau (Berlin) for SEM and Dr. W. Heink (Leipzig) for the development of the sophisticated NMR pulse spectrometer used in the self-diffusion measurements. We thank a referee for bringing to our attention ref. 24.

REFERENCES

1 M. Guisnet, P. Magnoux and C. Canaff, in Y. Murakami, A. Iijima and J.W. Ward (Eds.), New Developments in Zeolite Science and Technology, Proc. 7th Int. Conf. Zeolites, Tokyo, 1986. Studies in Surface Science and Catalysis, Vol. 28, Elsevier, Amsterdam, 1986, p. 701.
2 M. Guisnet, P. Magnoux and C. Canaff, Chemical Reactions in Organic and Inorganic Constraint Systems, D. Reidel Publ. Comp., Dordrecht, 1986, p. 131.
3 H. Schulz, W. Böhringer, W. Baumgartner and Zhao Siwei, in Y. Murakami, A. Iijima and J.W. Ward (Eds.), New Developments in Zeolite Science and Technology, Proc. 7th Int. Conf. Zeolites, Tokyo 1986, Studies in Surface Science and Catalysis, Vol. 28, Elsevier, Amsterdam, 1986, p. 915.
4 G.D. McLellan, R.F. Parker, R.F. Hower and D.M. Bibby, J. Catal., 99 (1986) 486.
5 V. Ducarme and J.C. Vedrine, Appl. Catal., 17 (1985) 175.
6 P. Dejaifve, A. Auroux, P.C. Gravelle, J.C. Vedrine, Z. Gabelica and E.G. Derouane, J. Catal., 70 (1981) 123.
7 D.H. Olson and W.O. Haag, ACS Symp. Ser., 248 (1984) 275.
8 R.H. Meinhold and D.M. Bibby, J. Catal., submitted.
9 D.M. Bibby, N.B. Milestone, J.E. Patterson and L.P. Aldrige, J. Catal., 97 (1986) 493.
10 J. Kärger, H. Pfeifer, J. Caro, M. Bülow, H. Schlodder, R. Mostowicz and J. Völter, Appl. Catal., 29 (1987) 21.

11 R.M. Lago, W.O. Haag, R.J. Mikovsky, D.H. Olson, S.D. Hellring, K.D. Schmitt and G.T. Kerr, in Y. Murakami, A. Iijima and J.W. Ward (Eds.), New Developments in Zeolite Science and Technology, Proc. 7th Int. Conf. Zeolites, Tokyo 1986, Studies in Surface Science and Catalysis, Vol. 28, Elsevier, Amsterdam, 1986, p. 677.
12 W.O. Haag, in D.H. Olson and A. Bisio (Eds.), Proc. 6th Int. Conf. Zeolites, Reno, 1983, Butterworths, Guildford, 1984, p. 466.
13 D.H. Olson, W.O. Haag and R.M. Lago, J. Catal., 61 (1980) 390.
14 S. Namba, K. Sato, K. Fujita, J.H. Kim and T. Yashima, in Y. Murakami, A. Iijima and J.W. Ward (Eds.), New Developments in Zeolite Sciences and Technology, Proc. 7th Int. Conf. Zeolites, Tokyo 1986, Studies in Surface Science and Catalysis, Vol. 28, Elsevier, Amsterdam, 1986, p. 661.
15 R.J. Argauer and G.P. Landolt, U.S. Patent 3 702 886 (1972).
16 J. Kärger, H. Pfeifer and W. Heink in D.H. Olson and A. Bisio (Eds.), Proc. 6th Int. Conf. Zeolites, Reno, 1983, Butterworths, Guildford, 1984, p. 184.
17 J. Kärger, AIChE J., 28 (1982) 417.
18 M. Bülow, Z. Chem., 25 (1985) 81.
19 J. Kärger, H. Pfeifer, J. Caro, M. Bülow, J. Richter-Mendau, B. Fahlke and L.V.C. Rees, Appl. Catal., 24 (1986) 187.
20 H. Pfeifer, D. Freude and M. Hunger, Zeolites, 5 (1985) 273.
21 R. Mostowicz and L.B. Sand, Zeolites, 3 (1983) 219.
22 D. Freude, M. Hunger, H. Pfeifer and W. Schwieger, Chem. Phys. Lett., 128 (1986) 62.
23 M.F. Post, J. van Amstel and H.W. Kouwenhoven, in D.H. Olson and A. Bisio (Eds.), Proc. 6th Int. Conf. Zeolites, Reno, 1983, Butterworths, Guildford, 1984, p. 517.
24 W.O. Haag, R.M. Lago and P.B. Weisz, Faraday Disc. Chem. Soc., 72 (1982) 317.
25 P. Ratnasamy, G.P. Babu, A.J. Chandwadkar and S.B. Kulkarni, Zeolites, 6 (1986) 98.
26 C. Herrmann, J. Haas and F. Fetting, Appl. Catal., 35 (1987) 299.
27 W. Hölderich and L. Riekert, Chem.-Ing. Techn., 58 (1986) 412.